*metals*

MDPI

*Article*

# Study of Influence of Aluminum Nitride Nanoparticles on the Structure, Phase Composition and Mechanical Properties of AZ91 Alloy

**Anton Khrustalyov [1], Ilya Zhukov [1], Pavel Nikitin [1,*], Vladislav Kolarik [2], Friedrich Klein [3], Anastasia Akhmadieva [1] and Alexander Vorozhtsov [1]**

[1] Faculty of Physics and Engineering, National Research Tomsk State University, 36 Lenin Ave, 634050 Tomsk, Russia; tofik0014@mail.ru (A.K.); gofra930@gmail.com (I.Z.); nas99.9@yandex.ru (A.A.); abv1953@mail.ru (A.V.)
[2] Department of Energetic Systems, Fraunhofer Institute for Chemical Technology, Joseph-von-Fraunhofer-Straße 7, 76327 Pfinztal, Germany; vladislav.kolarik@ict.fraunhofer.de
[3] Aalener Gesellschaft fuer Leichtbauteile mbH, Schleiermacherstraße 20, 73431 Aalen, Germany; Friedrich.Klein@aage-leichtbauteile.de
* Correspondence: upavelru@yandex.ru

**Abstract:** In this work, magnesium-based composites were obtained by shock-wave compaction of a powder mixture of Mg-5 wt.% AlN at a shock-wave pressure of 2 GPa. Their microstructure was investigated and the phase composition was determined, from which it follows that the nanoparticles retain their phase composition and are uniformly distributed in the magnesium matrix. The materials obtained by shock-wave compaction were used as master alloys for the production of magnesium alloys by die casting. The amount of aluminum nitride nanoparticles in the AZ91 magnesium alloy was 0.5 wt.%. Studies of the microstructure of the magnesium alloys showed a decrease in the average grain size of the magnesium matrix from 610 to 420 µm. Studies of mechanical properties have shown that the introduction of aluminum nitride nanoparticles increases the yield strength from 55 to 119 MPa, the tensile strength from 122 to 171 MPa and the plasticity from 4 to 6.5%, respectively. The effect of nanoparticles on the fracture behavior of the magnesium alloy under tension was determined.

**Keywords:** magnesium alloys; AZ91; LMMC; nanoparticles; aluminum nitride



**Citation:** Khrustalyov, A.; Zhukov, I.; Nikitin, P.; Kolarik, V.; Klein, F.; Akhmadieva, A.; Vorozhtsov, A. Study of Influence of Aluminum Nitride Nanoparticles on the Structure, Phase Composition and Mechanical Properties of AZ91 Alloy. *Metals* **2022**, *12*, 277. https://doi.org/10.3390/met12020277

Academic Editor: Shusen Wu

Received: 22 December 2021
Accepted: 27 January 2022
Published: 2 February 2022



## 1. Introduction

Light metal matrix composites (LMMCs) reinforced with dispersed particles have been actively studied in recent years as a new class of materials, with the aim of their possible application in mechanical engineering, aviation and other industries. Interest in such materials has arisen due to the unique combination of properties: high specific stiffness and strength, fracture toughness, electrical and thermal conductivity, wear resistance, hardness, durability, etc. [1–4]. As a matrix, it is possible to use such metals as aluminum, magnesium, titanium, nickel and their alloys. In this case, as strengthening particles, it is possible to use various ceramic and intermetallic particles (SiC, $Al_2O_3$, AlN, $Al_3Ni$, $Mg_2Si$, etc.) of different dispersion. There are many methods for obtaining metal-matrix composites [5], of which the most versatile and relatively simple to implement is casting, during which nanoparticles are introduced into the metal melt using a mechanical mixer [6]. The modern development of the aerospace and automotive industry determines a high demand for magnesium alloys, which combine a low density (1.8 g/cm$^3$), high specific strength and high performance in absorbing vibration loads. The most widely used casting magnesium alloy is AZ91, which belongs to the magnesium–aluminum–zinc–manganese system. The main reinforcing element in this alloy is aluminum. The chemical composition of such alloys is usually the following composition of elements: Mg—89.1–92.15%, Fe—up to 0.06%,

Si—up to 0.25%, Mn—0.15–0.5%, Ni—up to 0.01%, Al—7.5–9%, Cu—up to 0.1%, Zr—up to 0.002%, Be—up to 0.002%, Zn—0.2–0.8%, impurities: other—0.1%; total—0.5%.

In [7–12], the methods for obtaining metal–matrix composites based on casting and wrought magnesium alloys, the results of studies of the conditions and mechanisms of heterogeneous nucleation of the required microstructure of the matrix are described in detail, and also data are presented on changes in mechanical characteristics under conditions of quasi-static deformation and fracture. As shown in these works, the microstructure of metal matrix composites (MMC) is determined by the interaction between the matrix and the strengthener. The main characteristics of the microstructure include: the type, size and distribution of the strengthening phases, the grain size of the matrix, the products of the interaction between the matrix and the strengthening phase, and microstructural defects. The mechanical properties of magnesium MMC largely depend on these factors. It is extremely important to consider the particle size of the strengthener. In the previous research [13], the effect of the size and volume fraction of SiC on the mechanical properties of a composite based on AZ91D is described. It was shown that the introduction of particles with a size of 15 μm increased the fatigue strength, and, on the contrary, the introduction of particles with a size of 52 μm decreased it. In previous research [14], a significant decrease in the grain size of the matrix of the AZ91 alloy, strengthened with 10 wt.% SiC particles, was also noted. The phenomenon of grain refinement is due to the heterogeneous nucleation of the primary phase on SiC particles and the limitation of crystal growth caused by the presence of SiC particles. The effect of heterogeneous crystallization is confirmed by the fact that a decrease in the particle size leads to a decrease in the grain size of the obtained MMC. In previous research [12], data were obtained for a metal-matrix magnesium–aluminum composition. It was shown that an increase in the proportion of AlN particles from 5 to 10 and 15 wt.%, respectively, with a size from 1 to 3 μm, leads to a decrease in the density and strength of the samples. In [7], the effect of AlN nanoparticles less than 100 nm in size on the structure and mechanical properties of the obtained composites based on the ML12 (Mg–Zr–Zn) magnesium alloy was investigated. The introduction of 1.5 wt.% AlN nanoparticles leads to a simultaneous increase in strength from 150 to 210 MPa and elongation from 7 to 18%. It was shown that the introduction of 0.75 wt.% and 1.5 wt.% AlN nanoparticles leads to a decrease in the matrix grain size from 450 μm to 230 μm and 120 μm, respectively. Similar results of studying a composite were obtained with the introduction of 1.5 wt.% AlN nanoparticles (<d> <5 μm) [15]. A decrease in the content of AlN nanoparticles to less than 0.75 wt.% will reduce the negative effect of the powder, such as the porosity of magnesium alloys, and will provide dispersed hardening of the metal matrix. Thus, the purpose of this work is to obtain metal-matrix samples based on the matrix of the AZ91 magnesium alloy, strengthened by 0.5 wt.% AlN nanoparticles, and to conduct a study of their structure and a determination of elastoplastic and strength characteristics during mechanical tests.

## 2. Materials and Methods

### *2.1. Powder Mixture*

Magnesium powder (MPF-4 (99.9 wt.%, SOMZ, Solikamsk, Russia)) and aluminum nitride nanopowder were used as initial powders in the work. Aluminum nitride was obtained using the method of electric explosion of wires (EWM) [16]. For deagglomeration of nanoparticles, a powder mixture of Mg-5 wt.% AlN was prepared. The mixing of the powders was carried out using a mechanical mixer for 15 min at a rotation speed of 5000 rpm. Before mixing, a suspension was prepared from a powder mixture of petroleum ether and stearic acid, used as a surfactant. After mixing, petroleum ether was removed from the powder mixture. The choice of the above method was due to the fact that it allows deagglomeration of non-metallic nanoparticles and promotes their uniform distribution by achieving a simultaneous process of dispersion and mixing in liquid media using a surfactant.

### *2.2. Obtaining the Mg–AlN Master-Alloy*

The Mg–AlN master-alloy was produced from the obtained powder mixture. Shock-wave compaction occurred under the action of detonation products of contact charges of an explosive, which was used as a detonating cord. In shock-wave compaction, the following condition was satisfied (DS-B, diameter 5.8 mm, detonation velocity not less than 6500 m/s). The shock-wave compaction scheme is shown in Figure 1. The Mg-5 wt.% AlN powder mixture was placed in an aluminum container 150 mm high, 12 mm in diameter and 1 mm thick, and then hermetically closed on both sides. A detonation cord was wound around the resulting container, and the process of shock-wave compaction was carried out in a special chamber (Figure 1). After shock-wave compaction, the Mg–AlN master-alloy was extracted from the aluminum shell by mechanical surface treatment.

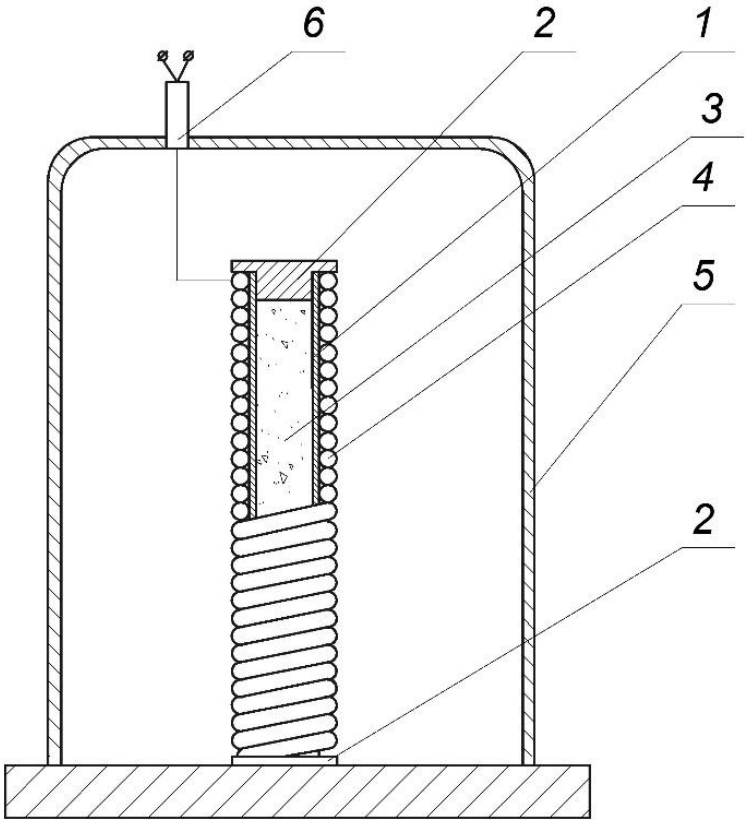


**Figure 1.** Scheme of obtaining the master alloy. 1—aluminum tube, 2—plug, 3—powder mixture, 4—detonating cord, 5—chamber wall, 6—electric detonator.

### *2.3. Casting Magnesium Alloys*

For casting, AZ91 magnesium alloy (89.1–92.15% Mg, 7.5–9% Al, 0.2–0.8% Zn, 0.15–0.5% Mn was used. The magnesium melt AZ91, previously prepared and heated to a temperature of 710 °C in an amount of 2000 g, was placed in a special steel crucible with a constant argon blowing. After that, the melt was mixed, and after 15 s, the Mg–AlN master-alloy was introduced with simultaneous mixing for 1 min at a mixer rotation speed of 500 rpm. The amount of AlN nanoparticles introduced into the melt was 0.5 wt.%. The obtained melt was poured into a cylindrical steel chill mold, which was subjected to vibration treatment during crystallization. The initial AZ91 alloy was manufactured with similar parameters: stirring and vibration treatment until complete crystallization without introducing nanoparticles.

### *2.4. Characterization*

The initial AlN nanoparticles were examined by transmission electron microscopy (TEM) using a Philips CM 30 microscope (Koninklijke Philips N.V., Amsterdam, Netherlands). The structures of the initial powders and the obtained materials were investigated using scanning electron microscopy (SEM) Philips SEM 515 (Koninklijke Philips N.V., Amsterdam, Netherlands) and optical microscopy Olympus GX71 Olympus Scientific Solutions Americas, Waltham, MA, USA). X-ray diffraction analysis of the master-alloy was performed using a Shimadzu XRD 6000 diffractometer (Shimadzu, Tsukinowa, Japan). The uniaxial tension experiments were performed on a dual column tabletop testing system Instron 3369 (Instron European Headquarters, High Wycombe, UK) with strain rate of 0.001 $s^{-1}$ and test temperature of 24°C, according to ISO 6892:1984. For testing, flat specimens with the dimensions of the working area were used: length 25 mm, width 6 mm and thickness 2 mm. For tensile tests, a minimum of three experiments were carried out for each alloy. A mechanical torsion test was also carried out in this work. Samples of the obtained alloys were subjected to torsion until fracture with simultaneous registration of the torque. Torsion tests were carried out on a minimum of three samples of each alloy. The torsion specimens were rods 100 mm long. The microhardness testing was performed on a Metolab 503 Vickers hardness tester (Metolab Company, Moscow, Russia) at an indentation load of 50 g. Each sample was measured at least 10 times.

## 3. Results and Discussion

### *3.1. Initial Powders*

Figure 2 shows a SEM image and a histogram of the particle size distribution of magnesium powder. The powder is composed of irregularly shaped particles (Figure 2a) with an average particle size of 90 μm (Figure 2b).

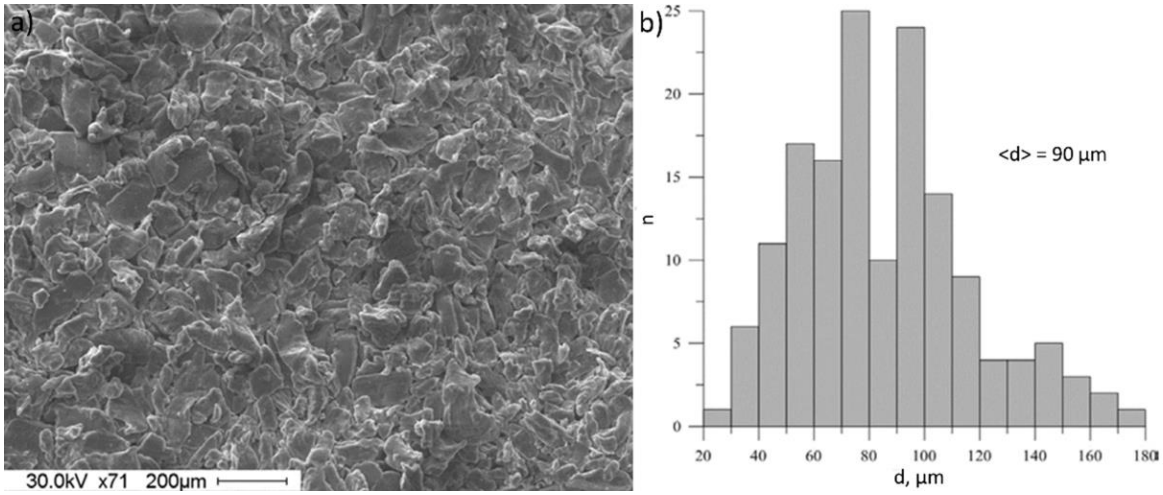


**Figure 2.** SEM image (**a**) and histogram of particle size distribution of the initial magnesium powder (**b**).

Figure 3 shows a TEM image of AlN nanoparticles (Figure 3a), a histogram of the nanoparticle size distribution (Figure 3b) and the mass distribution of the powder (Figure 3c). The particle size is in the range from 0.07 μm to 0.2 μm, with the probabilistic size $\tilde{a}_n$ = 38 nm, average size over the surface $\tilde{a}_s$ = 57 nm and average mass size $\tilde{a}_m$ = 76 nm.

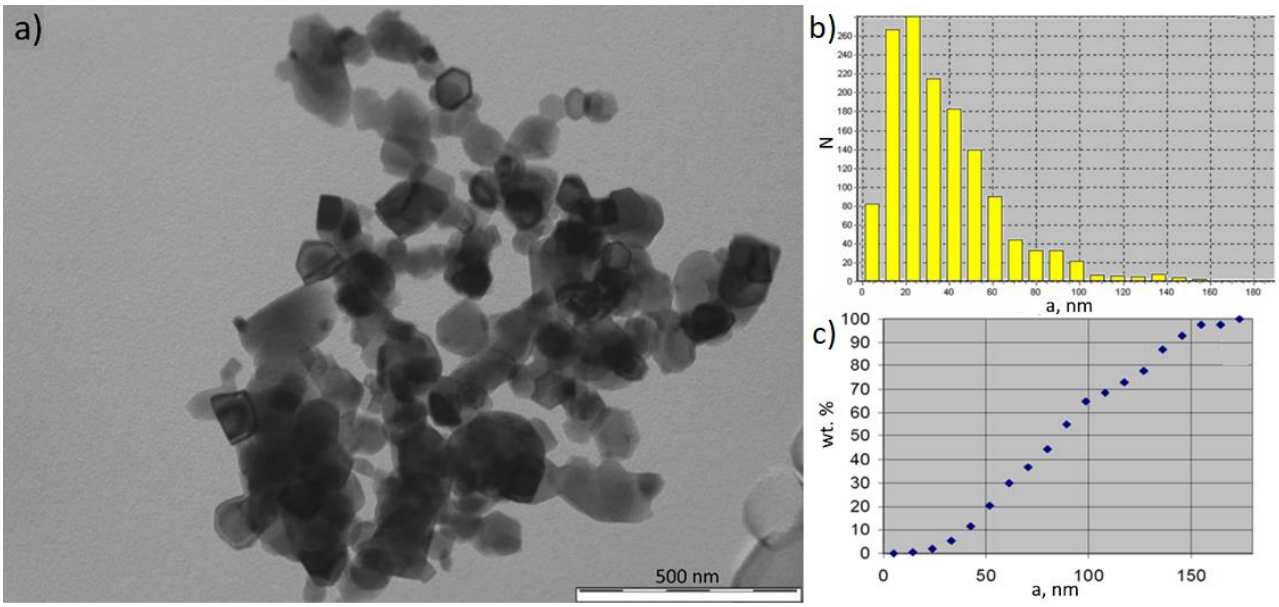


**Figure 3.** TEM image of AlN nanoparticles (**a**), histogram of particle size distribution (**b**) and integral curve mass distribution of particles (**c**).

### *3.2. Mg–AlN Master-Alloy*

There is a clear boundary between the master-alloy and its shell, and the master-alloy does not have large defects after shock-wave compaction. Energy dispersive analysis of the master-alloy (Figure 4a) showed that the material consists mainly of magnesium—94 wt.% (matrix) and oxygen—3 wt.%, which is present in the raw magnesium powder. In addition, the composite contains 1 wt.% nitrogen and 2 wt.% aluminum, which may indicate that aluminum nitride retains its original structure after shock-wave compaction. As can be seen from the SEM images (Figure 4b), the magnesium grains were significantly deformed during the shock-wave compaction. At the same time, their average size did not change in comparison with the average grain size of the initial powder, and it was also about 90 µm. The SEM images also show the stratification of the material along the boundaries of the magnesium grains. This may be due to the fact that, during the preparation of powder mixtures on the surface of some magnesium particles, nanoparticles are nevertheless combined into agglomerates, which complicates the sintering process at grain boundaries. At higher resolution (Figure 4c), nanoparticles are visible in the master-alloy, presented as light inclusions. Some of the nanoparticles agglomerated, but the average size of the agglomerates does not exceed 500 nm. To determine the composition of nanoparticles, the obtained SEM image was mapped (Figure 4d–f). According to the results obtained, the grain body contains aluminum nitride nanoparticles. The highest content of aluminum and nitrogen was found in areas with defects at the boundaries of magnesium grains (Figure 4e,f), which also confirms the imperfection of the obtained material.

XRD analysis showed that the content of the aluminum nitride phase in the master-alloy is 4 wt.%. Phase and structural parameters of the Mg–AlN master-alloy are presented in Figure 5 and Table 1.

| Element | Wt% | At% |
|---|---|---|
| N | 00.93 | 01.58 |
| O | 02.86 | 04.26 |
| Mg | 93.97 | 92.17 |
| Al | 02.25 | 01.99 |

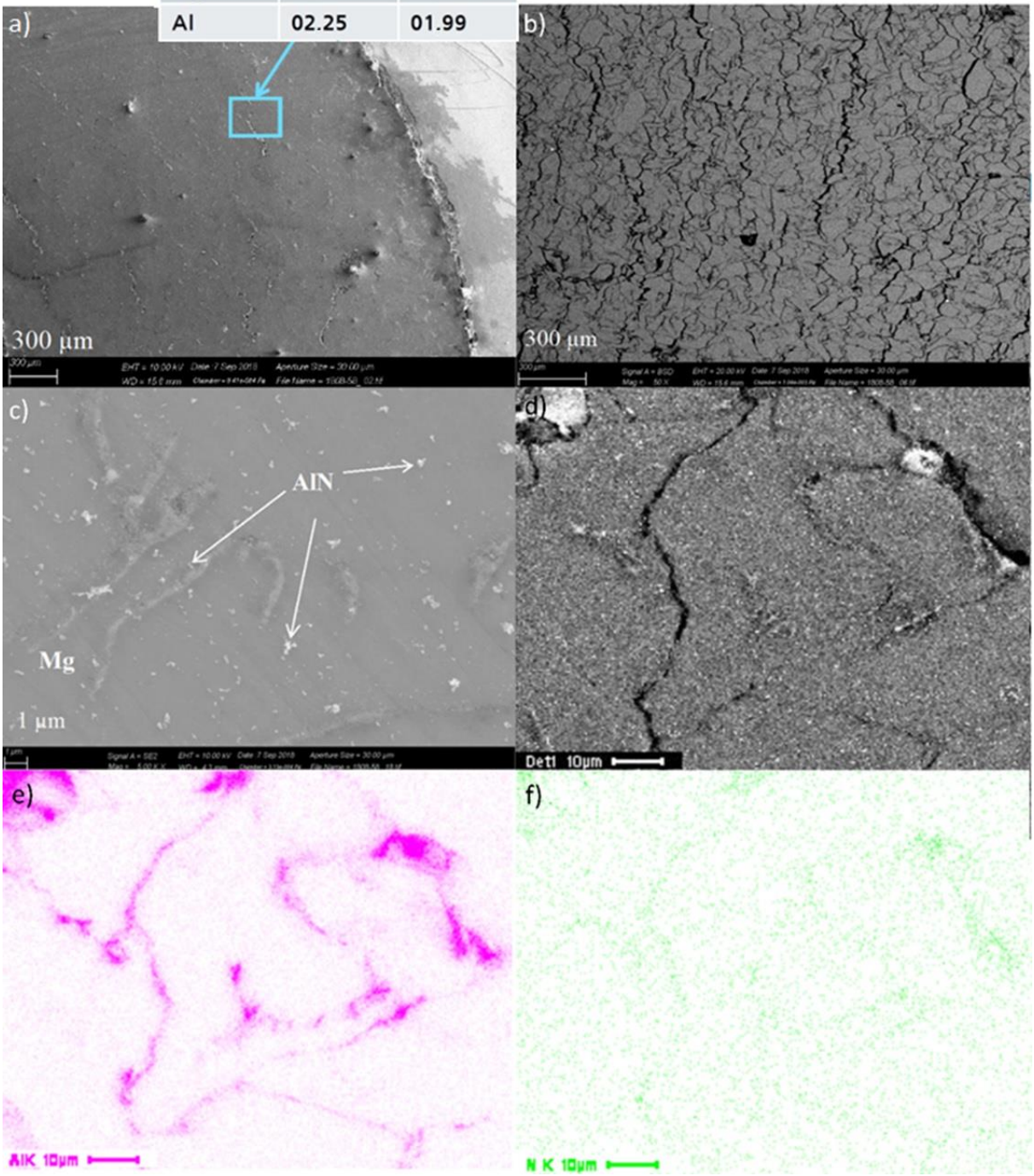


**Figure 4.** SEM images at ×100 (**a**), ×200 (**b**), ×1000 (**c**) magnifications and mapping (SEM image (**d**), Al (**e**), N (**f**)) of the Mg–AlN master-alloy.

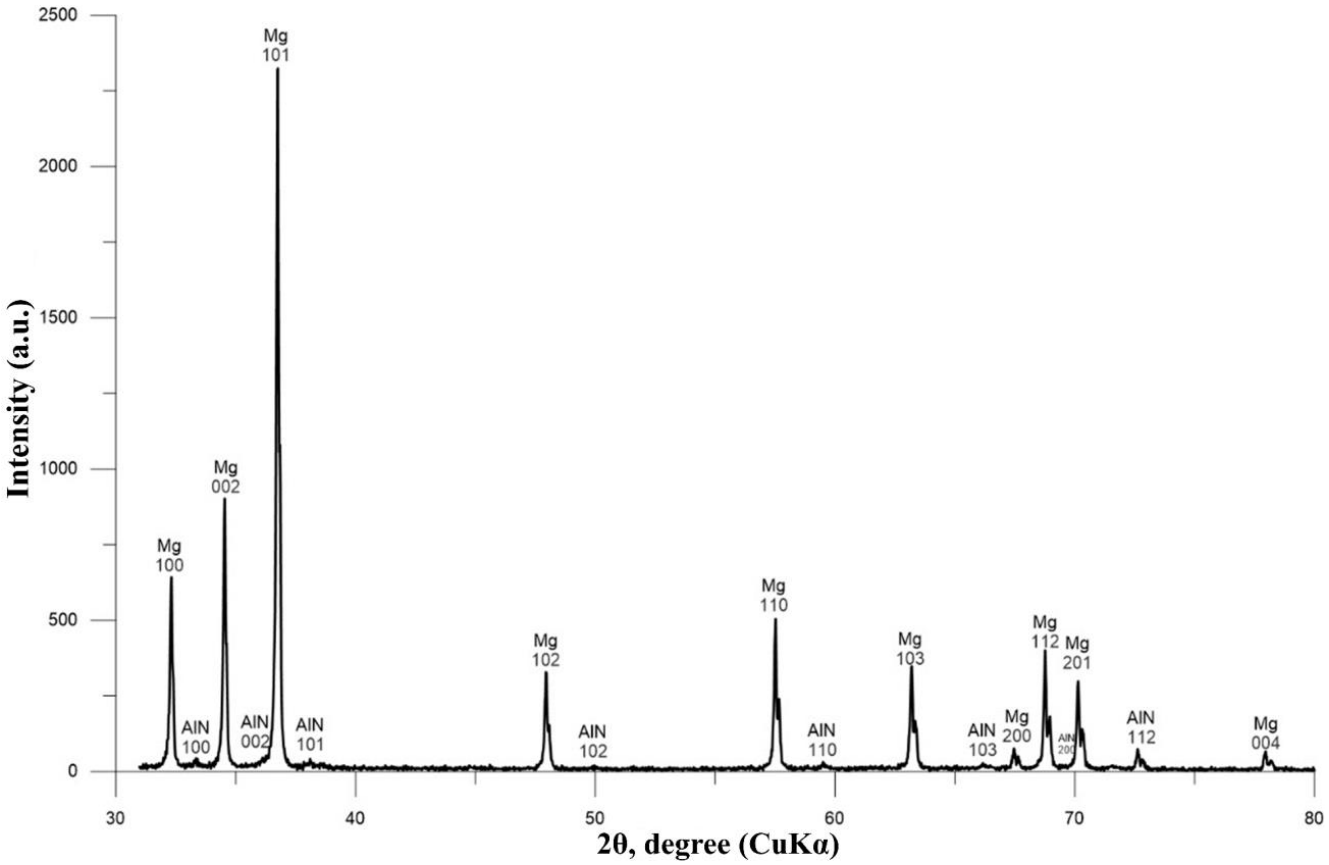


**Figure 5.** XRD pattern of the Mg–AlN master-alloy.

**Table 1.** Phase and structural parameters of the Mg–AlN master-alloy.

| Phase | Phase Content, wt.% | Lattice Parameters, Å | CSR Size, nm | $\Delta d/d*10^{-3}$ |
|---|---|---|---|---|
| Mg | 96 | a = 3.2101<br>c = 5.2112 | 86 | 0.5 |
| AlN | 4 | a = 3.1103<br>c = 4.9848 | 53 | 0.5 |

### *3.3. AZ91–AlN Alloy*

Figure 6 shows SEM (Figure 6a,b) and optical (Figure 6c,d) images of the microstructure of AZ91 magnesium alloys. As can be seen from the obtained images, no large pores are observed in the structure of the initial AZ91 alloy (Figure 6a,c), and the porosity does not exceed 5%. The introduction of AlN nanoparticles leads to a slight increase in porosity, up to 7% (Figure 6b,d). Apparently, the increase in porosity is due to the introduction of an additional volume of gas with the introduction of the Mg–AlN master alloy (Figure 6b).

At the same time, in the structure of the AZ91–AlN alloy (Figure 6b), large pores and undissolved master-alloy elements are also not observed, which, as a rule, occurs during sintering of agglomerates in the matrix and the impossibility of their further dissolution during alloy casting [17,18]. In the structure of the AZ91–AlN alloy, non-metallic inclusions are observed, which can be agglomerates of introduced nanoparticles sintered from smaller particles observed in the initial Mg–AlN master-alloy (Figure 4c) and contained in nitrogen-supersaturated master-alloy defects (Figure 4f). X-ray phase analysis of the resulting alloys allows for determination of the phase of aluminum nitride in the AZ91–AlN alloy (Figure 7). It can be seen that the introduction of the Mg–AlN master-alloy does not lead to a change in the phase composition of the metal matrix.

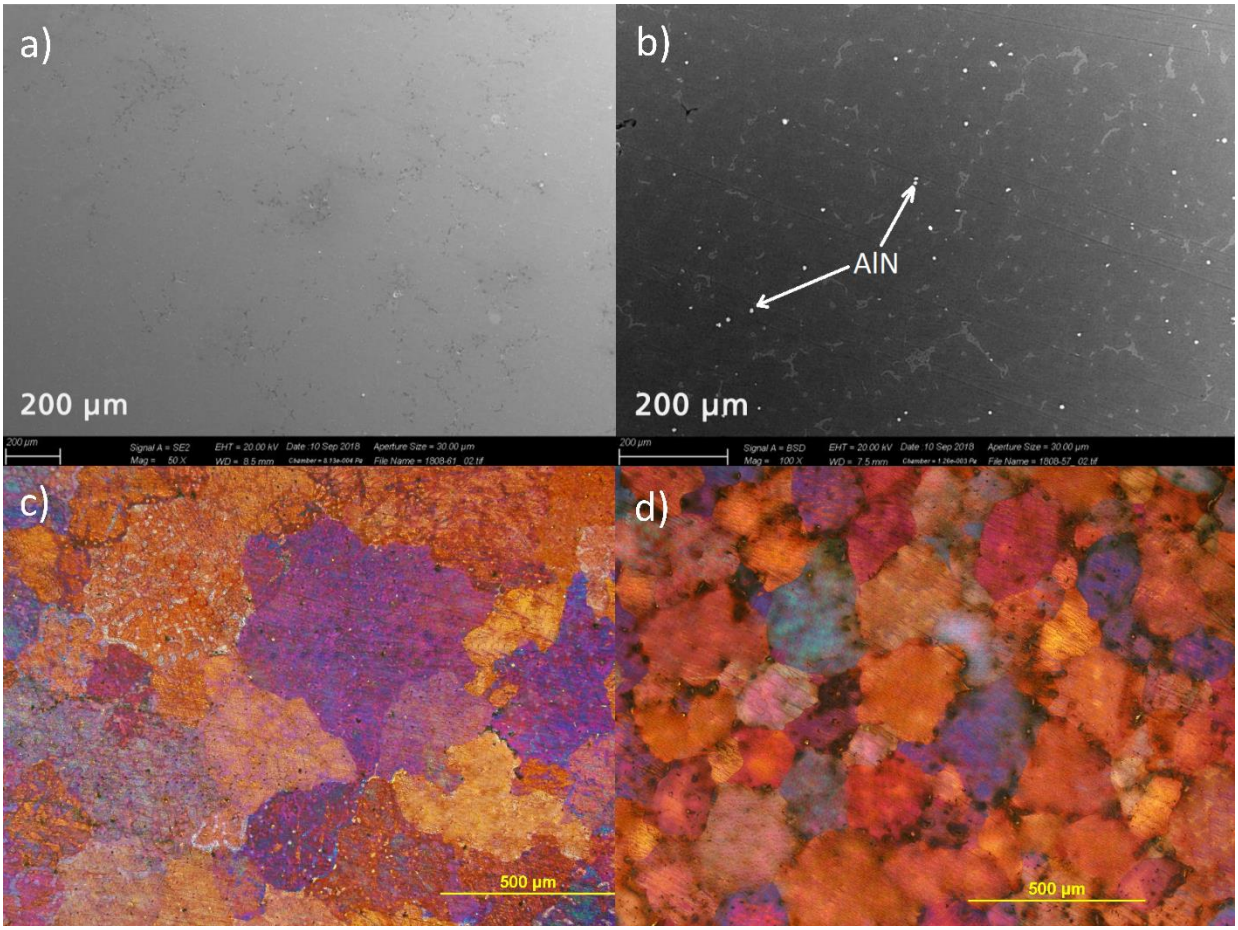


**Figure 6.** SEM (**a**,**b**) and optical (**c**,**d**) images of the structure of magnesium alloys AZ91 (**a**,**c**), AZ91-AlN (**b**,**d**).

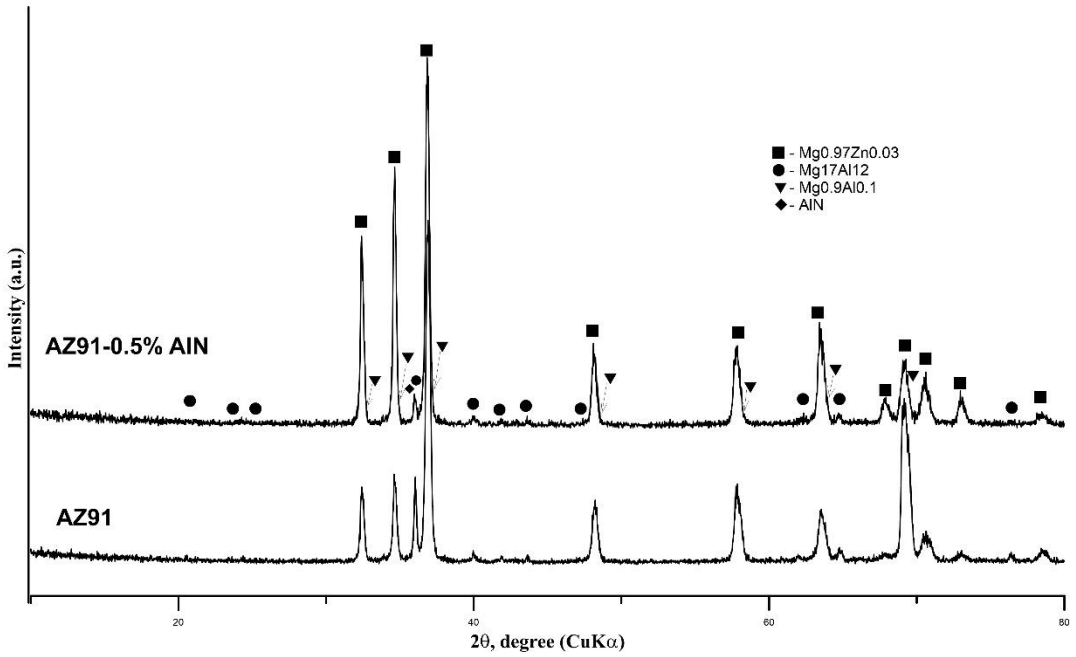


**Figure 7.** XRD pattern of the AZ91 magnesium alloys.

Aluminum nitride nanoparticles have a modifying effect on the microstructure of the AZ91 alloy. It was found that, with the introduction of 0.5 wt.% AlN, the average grain size of the magnesium alloy decreases from 490 to 310 μm. The grain refinement is due to the heterogeneous nucleation of the primary phase on AlN particles and the limitation of crystal growth caused by the presence of AlN particles [19–21]. A change in the phase composition after the introduction of the master-alloy could also affect the grain size, however, according to the XRD data (Figure 7), this phase composition did not change. The modification effect occurs due to the similarity of the crystal lattice parameters of aluminum and magnesium nitride (Table 1). In previous research [19], it was shown that the introduction of aluminum nitride microparticles (5 μm) leads to a decrease in the average grain size of a magnesium alloy containing 3 wt.% Al. In this case, the highest efficiency was achieved with the introduction of 0.5 wt.% aluminum nitride: the average grain size decreased from 450 to 110 μm. From the point of view of modifying the structure, nanoparticles demonstrate lower efficiency compared to microparticles [19]. To estimate the amount of particles introduced into the melt, a calculation was made using the following formula:

$$N_p = \frac{Vp}{\pi r^3}$$

where $r$ is the radius of the particles (2.5 μm for the alloy [19] and 40 nm for the alloy obtained in this work) and $V_p$ is the volume of particles, determined by the formula:

$$V_p = V_a - V_m$$

where $V_a$ is the total volume of the alloy (for the calculation, the conditional volume of 57.535 g/cm$^3$, corresponding to the mass of 100 g, was used) and $Vm$ is the volume of the matrix.

For the alloy [19], the calculated amount of particles was 1.28 × 10$^9$ pieces/100 g, while for the obtained AZ91–AlN alloy, this amount was about 200 trillion pieces/100 g. Thus, the number of crystallization centers in the obtained alloys was approximately 156 thousand times more than necessary and sufficient for effective modification of the alloy structure. However, the main part of aluminum nitride nanoparticles can act as strengtheners, initiating the Orowan mechanisms and load distribution in a "soft" metal matrix [21].

Measurements of the microhardness of the resulting alloys showed that the introduction of nanoparticles does not lead to its increase, which was 59 ± 6 HV for the initial AZ91 alloy and 58 ± 8 HV for the AZ91–AlN alloy. Tensile stress–strain curves for the parent and alloyed alloys are shown in Figure 8. The results of tensile mechanical tests are shown in Table 2.

**Table 2.** Mechanical properties of AZ91 magnesium alloys after tensile tests.

| Alloy | $YS_{tension}$, MPa | $UTS_{tension}$, MPa | $\delta_{tension}$, % |
|---|---|---|---|
| AZ91 | 65 ± 4 | 176 ± 6 | 6 ± 0.4 |
| AZ91–AlN | 53 ± 3 | 214 ± 9 | 10 ± 0.5 |

It was found that the introduction of aluminum nitride nanoparticles leads to an increase in the strength and plasticity of the magnesium alloy from 176 to 214 MPa and from 6 to 10%, respectively. The obtained results are in good agreement with previous studies [22]. A significant contribution to the increase in mechanical properties could be made by the refinement of the grain of the alloy [23] according to the Hall–Petch law, however, this mechanism provides for a direct effect of the grain size on the yield stress [24], which does not increase. It is assumed that the introduction of particles into the grain body can lead to a deviation of a potential crack from the grain boundary into its volume, as well as to a greater involvement of the metal matrix in the process of deformation and fracture [21,22].

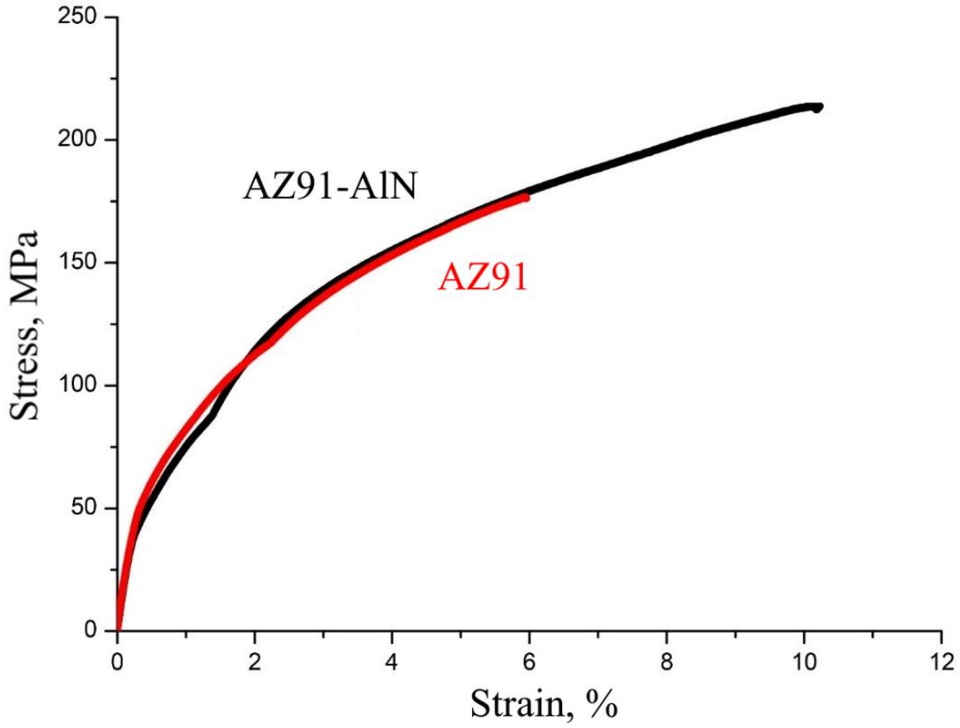


**Figure 8.** Tensile diagrams of AZ91 magnesium alloys.

Taking into account the equiaxiality of the grains of the magnesium alloy and aluminum nitride particles, experiments on the torsion of the obtained magnesium alloys were performed (Table 3). As can be seen from Table 3, the introduction of aluminum nitride nanoparticles made it possible to increase the yield strength from 63 to 73 MPa, the ultimate strength from 130 to 176 MPa and the ductility from 4.6 to 11.2%, respectively, of the AZ91 magnesium alloy during torsion. Thus, there is a lack of anisotropy in the mechanical properties of the strengthened magnesium alloys, which can equally prevent fracture at normal and tangential stresses due to the equiaxiality of the introduced nanoparticles and grains of the AZ91 alloy.

**Table 3.** Mechanical properties of AZ91 magnesium alloys after torsion tests.

| Alloy | $YS_{torsion}$, MPa | $UTS_{torsion}$, MPa | $\delta_{torsion}$, % |
|---|---|---|---|
| AZ91 | 63 ± 7 | 130 ± 9 | 4.6 ± 0.2 |
| AZ91–AlN | 73 ± 4 | 176 ± 8 | 11.3 ± 0.4 |

The reduction in cracking due to the introduction of nanoparticles is confirmed by studies of the fracture surface of the obtained magnesium alloys (Figure 9). In the initial alloy, AZ91, the fracture has a ductile–brittle character (Figure 9a). However, with the introduction of aluminum nitride nanoparticles in the AZ91 alloy, there is a significant change in the fracture surface, which, despite the preservation of the ductile–brittle nature, has a more complex geometry (Figure 9c), which can contribute to a simultaneous increase in the tensile strength and ductility of the magnesium alloy (Tables 2 and 3). The fracture surfaces have a dimple structure, which also indicates the predominance of the ductile fracture mechanism. Dendrites can be seen at the fracture surface (Figure 9b,d). In the initial AZ91 alloy (Figure 9b), deformation bands are observed, the lines of which are perpendicular to the interface between the dendrites, which can act as potential lines of cracking of the alloy.

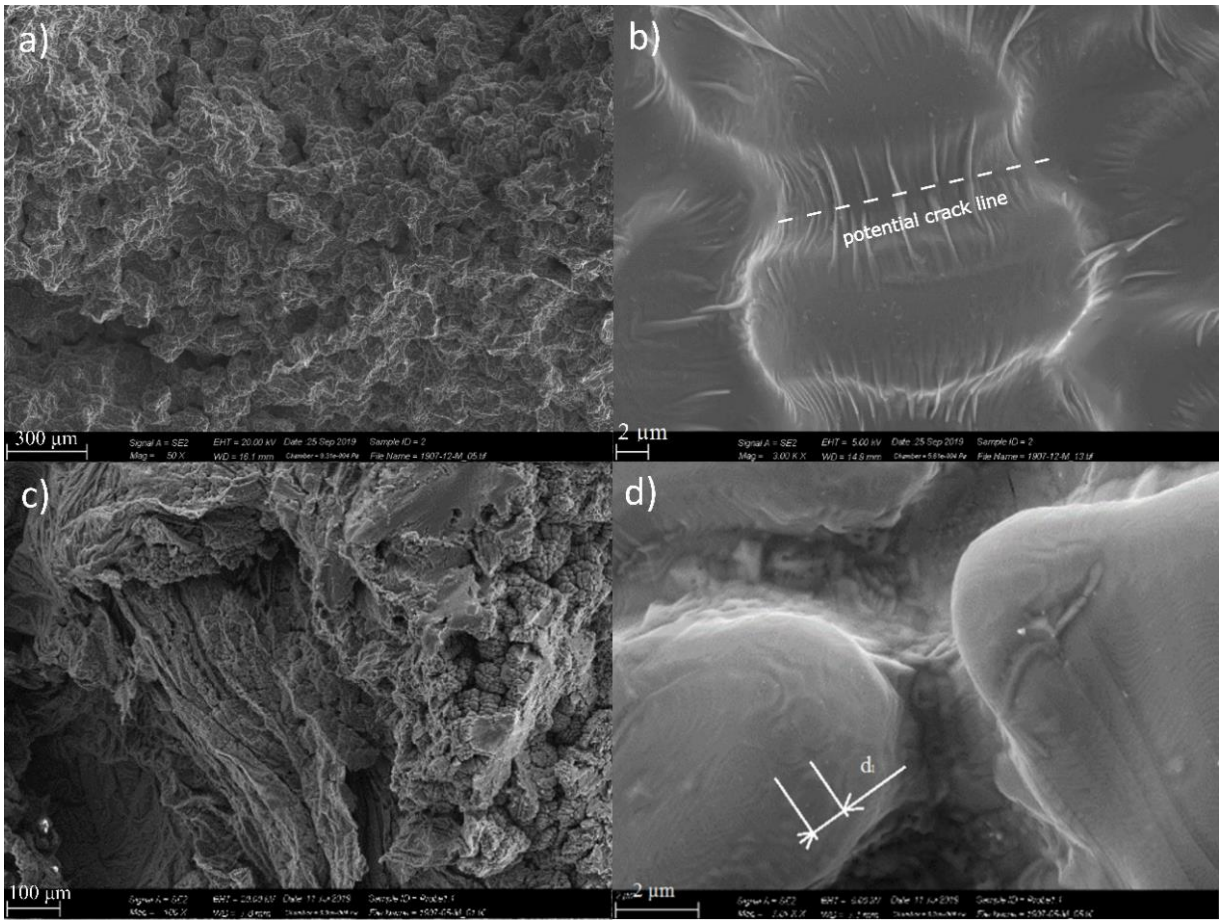


**Figure 9.** SEM images of the fracture surface of the AZ91 (**a**,**b**) and AZ91–AlN (**c**,**d**) magnesium alloy. Where $d_l$ - The average size of the ring-shaped areas of deformation.

In turn, the introduction of aluminum nitride nanoparticles made it possible to significantly change the dendrite deformation. Figure 9d shows that the deformation lines are ring-shaped, with an average size of approximately 1 μm ($d_l$). Nanoparticles, the average size of which is approximately 80 nm, can serve as a source of these rings, thereby uniformly distributing stresses within the magnesium matrix, avoiding early cracking between dendrites.

## 4. Conclusions

In this work, the microstructure and properties of the AZ91 magnesium alloy reinforced with aluminum nitride nanoparticles were investigated. AlN nanoparticles were introduced using the Mg–AlN master-alloy obtained by shock-wave compaction. It was found that the introduction of AlN nanoparticles leads to an insignificant increase in the porosity of the magnesium alloy from 5 to 7% and has a modifying effect on the microstructure, reducing the average grain size of the alloy from 490 to 310 μm. The results of tensile tests showed that the introduction of aluminum nitride nanoparticles leads to an increase in the ultimate strength and plasticity of the AZ91 magnesium alloy from 176 to 214 MPa and from 6 to 10%, respectively. The results of torsion tests showed that the introduction of aluminum nitride nanoparticles leads to an increase in the yield stress, ultimate strength and plasticity of the AZ91 magnesium alloy from 63 to 73 MPa, from 130 to 176 MPa and from 4.6 to 11.2%, respectively. Analysis of fracture surfaces showed that the introduction of AlN nanoparticles promotes ductile–brittle fracture of the alloy and a uniform distribution of stresses within the matrix.

**Author Contributions:** Conceptualization, I.Z. and A.K.; methodology, V.K., F.K. and A.A.; investigation, V.K. and A.A.; writing—original draft preparation, P.N. and I.Z.; supervision, A.V.; funding acquisition, I.Z. All authors have read and agreed to the published version of the manuscript.

**Funding:** This work was carried out with financial support from the Ministry of Education and Science of the Russian Federation (State assignment No. FSWM-2020-0028).

**Data Availability Statement:** The data presented in this study are available in the article.

**Acknowledgments:** This work was supported by the Ministry of Science and Higher Education of the Russian Federation in the framework of agreement dated 07/26/2021 no. 075-15-2021-693 (no. 13.ЦКП.21.0012).

**Conflicts of Interest:** The authors declare no conflict of interest.

## References

1. Kim, C.S.; Sohn, I.; Nezafati, M.; Ferguson, J.B.; Schultz, B.F.; Bajestani-Gohari, Z.; Rohatgi, P.K.; Cho, K. Prediction models for the yield strength of particle-reinforced unimodal pure magnesium (Mg) metal matrix nanocomposites (MMNCs). *J. Mater. Sci.* **2013**, *48*, 4191. [CrossRef]
2. Rohatgi, P.K.; Schultz, B. Lightweight Metal Matrix Nanocomposites–Stretching the Boundaries of Metals. *Mater. Matters* **2007**, *4*, 16–21.
3. Muley, A.V.; Aravindan, S.; Singh, I.P. Nano and hybrid aluminum based metal matrix composites: An overview. *Manuf. Rev.* **2015**, *2*, 15. [CrossRef]
4. Casati, R.; Vedani, M. Metal Matrix Composites Reinforced by Nano-Particles—A Review. *Metals* **2014**, *4*, 65–83. [CrossRef]
5. Kurganova, Y.A.; Kolmakov, A.G. *Konstrukcionnye Metallomatrichnye Kompozicionnye Materialy: Uchebnoe Posobie*; Publishing House of MSTU im. N.E.: Bauman, Moscow, 2015; p. 141. (In Russian)
6. Ye, H.Z.; Liu, X.Y. Review of recent studies in magnesium matrix composites. *J. Mater. Sci.* **2004**, *39*, 6153–6171. [CrossRef]
7. Khrustalyov, A.P.; Vorozhtsov, S.A.; Zhukov, I.A.; Promakhov, V.V.; Dammer, V.K.; Vorozhtsov, A.B. Structure and mechanical properties of magnesium-based composites reinforced with nitride aluminum nanoparticles. *Russ. Phys. J.* **2017**, *59*, 2183–2185. [CrossRef]
8. Vorozhtsov, S.; Khrustalyov, A.; Khmeleva, M.; Zhukov, I. Structure and deformation characteristics in magnesium alloy ZK51A reinforced with AlN nanoparticles. *AIP Conf. Proc.* **2016**, *1772*, 030004. [CrossRef]
9. Sazonov, M.A.; Chernishova, T.A.; Rokhlin, L.L. Particulate-reinforced magnesium matrix composite: Production and properties (review). *Konstr. I Funkc. Mater.* **2010**, *2*, 3–22. (In Russian)
10. Ferguson, J.B.; Sheykh-Jaberi, F.; Kim, C.S.; Rohatgi, P.K.; Cho, K. On the strength and strain to failure in particle-reinforced magnesium metal-matrix nanocomposites (Mg MMNCs). *Mater. Sci. Eng. A* **2012**, *558*, 193–204. [CrossRef]
11. Gupta, M.; Wong, W.L.E. Magnesium-based nanocomposites: Lightweight materials of the future. *Mater. Charact.* **2015**, *105*, 30–46. [CrossRef]
12. Chen, J.; Bao, C.; Chen, W.; Zhang, L.; Liu, J. Mechanical properties and fracture behavior of Mg-Al/AlN composites with different particle contents. *J. Mater. Sci. Technol.* **2017**, *33*, 668–674. [CrossRef]
13. Vaidya, A.R.; Lewandowski, J.J. Effects of SiCp size and volume fraction on the high cycle fatigue behavior of AZ91D magnesium alloy composites. *Mater. Sci. Eng. A* **1996**, *220*, 85–92. [CrossRef]
14. Luo, A. Development of matrix grain structure during the solidification of a Mg (Az91)/SiCp composite. *Scr. Metall. Mater.* **1994**, *31*, 1253. [CrossRef]
15. Cao, G.; Choi, H.; Oportus, J.; Konishi, H.; Li, X. Study on tensile properties and microstructure of cast AZ91D/AlN nanocomposites. *Mater. Sci. Eng. A* **2008**, *494*, 127–131. [CrossRef]
16. Lerner, M.; Vorozhtsov, A.; Guseinov, S.; Storozhenko, P. *Metal Nanopowders: Production Characterization, and Energetic Applications*; Gromov, A.A., Teipel, U., Eds.; Wiley-VCH: Weinheim, Germany, 2014; pp. 79–106.
17. Naydenkin, E.; Mishin, I.; Khrustalyov, A.; Vorozhtsov, S.; Vorozhtsov, A. Influence of Combined Helical and Pass Rolling on Structure and Residual Porosity of an AA6082-0.2 wt% $Al_2O_3$ Composite Produced by Casting with Ultrasonic Processing. *Metals* **2017**, *7*, 544. [CrossRef]
18. Vorozhtsov, S.; Minkov, L.; Dammer, V.; Khrustalyov, A.; Zhukov, I.; Promakhov, V.; Vorozhtsov, A.; Khmeleva, M. Ex situ introduction and distribution of nonmetallic particles in aluminum melt: Modeling and experiment. *JOM.* **2017**, *69*, 2653–2657. [CrossRef]
19. Fu, H.M.; Zhang, M.X.; Qiu, D.; Kelly, P.M.; Taylor, J.A. Grain refinement by AlN particles in Mg–Al based alloys. *J. Alloys Compd.* **2009**, *478*, 809–812. [CrossRef]
20. Sheng, L.Y.; Yang, F.; Xi, T.F.; Guo, J.T.; Ye, H.Q. Microstructure evolution and mechanical properties of $Ni_3Al/Al_2O_3$ composite during self-propagation high-temperature synthesis and hot extrusion. *Mater. Sci. Eng. A* **2012**, *555*, 131–138. [CrossRef]
21. Dieringa, H.; Katsarou, L.; Buzolin, R.; Szakács, G.; Horstmann, M.; Wolff, M.; Mendis, C.; Vorozhtsov, S.; StJohn, D. Ultrasound Assisted Casting of an AM60 Based Metal Matrix Nanocomposite, Its Properties, and Recyclability. *Metals* **2017**, *7*, 388. [CrossRef]

22. Khrustalyov, A.P.; Garkushin, G.V.; Zhukov, I.A.; Razorenov, S.V.; Vorozhtsov, A.B. Quasi-Static and Plate Impact Loading of Cast Magnesium Alloy ML5 Reinforced with Aluminum Nitride Nanoparticles. *Metals* **2019**, *9*, 715. [CrossRef]
23. Sheng, L.Y.; Yang, F.; Guo, J.T.; Xi, T.F.; Ye, H.Q. Investigation on NiAl–TiC–$Al_2O_3$ composite prepared by self-propagation high temperature synthesis with hot extrusion. *Compos. Part B Eng.* **2013**, *45*, 785–791. [CrossRef]
24. Petch, N. The cleavage strength of polycrystals. *J. Iron Steel Inst.* **1953**, *174*, 25–28.